RSC Advances

ROYAL SOCIETY OF CHEMISTRY

www.rsc.org/advances

Cite this: DOI:

www.rsc.org/advances

Full Paper

The synthesis and characterization of carboxybetaine functionalized polysiloxanes for the preparation of anti-fouling surfaces

Liujun Cheng,[a] Qiongqiong Liu,[a] Yufeng Lei,[a] Yaling Lin,[b,*] Anqiang Zhang[a,*]

Received (in XXX, XXX) Xth XXXXXXXXX 2014, Accepted Xth XXXXXXXXX 2014

DOI:

The nonspecific protein adsorption and bacterial adhesion caused serious problems in biomedical devices, marine engineering, membrane separation and many other areas. In order to develop a water-soluble bio-adhesion resistant material, a series of novel zwitterionic polymers, carboxybetaine functionalized polysiloxanes (PDMS-g-CB), were synthesized via a three-step procedure. FT-IR and NMR were used to characterize the chemical structures of PDMS, and the solution properties (i.e. CMC) and biological characteristics were investigated. The high biocompatibility of PDMS-g-CB was demonstrated by hemolysis assay, skin irritation evaluation and acute oral toxicity testing. To evaluate the anti-fouling properties and hydrophilic properties of PDMS-g-CB, PDMS-g-CB was blending with PDMS elastomer to form films (b-PDMS). Water contact angle and ATR-FTIR measurements revealed that the hydrophobic PDMS surfaces converted to hydrophilic surfaces after the introducing of PDMS-g-CB. The anti-fouling properties of b-PDMS were evaluated by protein adsorption and bacterial adhesion test. Results showed that the amount of adsorbed protein and bacteria adhesion were significantly reduced compared with the untreated PDMS. These finding suggest that PDMS-g-CB are biocompatible and promising materials for the construction of anti-fouling surfaces.

Keywords: carboxybetaine, polysiloxanes, protein adsorption, bacterial adhesion, anti-fouling, biocompatibility

1 INTRODUCTION

Over the past few decades, chemical pesticides play a pivotal role for pest management in agriculture. Although pesticides proved to be reliable and effective pest control agents, they also causing undesirable ecological and economic consequences for our lives, such as insecticide resistance, outbreaks of secondary pests, increased health risks to humans and livestock, destruction of natural environment. [1, 2] Therefore, a growing emphasis is on reducing the use of chemical pesticides. To overcome those problems, continuous efforts have been made to develop a harmless way for pest management, which has little adverse impact on human health and harmless to the environment. [3, 4]

It was noticed that the effective adsorption of protein on the material surface is the fundament of the attachment, survival and reproduction of phytophagous insects on plant surface, [5] if this process could be regulated by changing the micro-environment of plant surface, we may control the pests in a harmless way. Thus, the constructions of low-fouling or non-fouling surfaces are highly desirable. For example, according to the normal procedure of phytophagous insect oviposition, the insect, such as *Spodoptera exigua* (beet armyworm), would secrete mucus in the abaxial leaf surface to help the adhesion of eggs, in which the mucus mainly containing water, protein and a small amount of carbohydrate. [6] We assume that if a non-toxic and protein adsorption resistant leaf surface was achieved by spraying a polymeric coating, the adhesion of eggs on leaf surface could be damaged or weaken, and the sprayed leave surface would be an unsuitable environment for pest to secret, thus pest control could be partly achieved without killing or deterring the pest.

Besides, there is a significant need for the development of anti-fouling materials to resist nonspecific protein adsorption and bacteria adhesion for implantable biomaterials, biosensors, ocean engineering and membrane separation application. [7-8]

To date, few materials can be used for construction of anti-fouling or non-fouling surfaces which could resist nonspecific protein adsorption effectively. Polyethylene glycol (PEG) and oligoethylene glycol (OEG) based materials are the most widely used anti-fouling materials, [9-11] studies show that PEG or OEG modified surface can reduce protein adsorption and cell adhesion to a large scale. Steric exclusion effect and surface hydration are considered as the key to the antifouling properties for PEG and OEG based materials, respectively. [12-14] However, PEG and OEG based materials belong to polyether which is susceptible to oxidation damage, especially in the presence of oxygen and transition metal ions. [15, 16] Recently, zwitterionic polymers, such as phosphorylcholine (PC), polysulfobetaine (pSB) and polycarboxybetaine (pCB), have attracted much attention due to their super low-fouling characteristics and relative stability. [17-19]

Jiang and co-workers had prepared several zwitterionic poly(carboxybetaine methacrylate) (pCBMA) modified surfaces, those surfaces showed highly resistant to nonspecific protein adsorption and bacterial adhesion. [20-22] It is believed that zwitterionic polymer modified surfaces could form a hydration layer near the surface via ionic solvation and hydrogen bonding, which would prevent the adsorption of protein by the hydration barrier. [23, 24]

In this study, in order to obtain a water-soluble, non-toxic and biocompatible polymer with excellent anti-fouling and film forming properties, we designed a novel carboxybetaine functionalized polymer (PDMS-g-CB). The polymer consisted of a PDMS backbone and carboxybetaine pendant-side, the PDMS backbone would endow the polymer with extremely low glass transition temperature, low surface tension, optically transparency, permeability to gas, durability, biocompatibility, and good film forming properties, while the introduction of carboxybetaine groups offer high resistance to protein adsorption and bacterial adhesion. And we could tailor the hydrophilicity and anti-fouling properties by adjusting the ratio of carboxybetaine pendant-side. The biocompatibility (i.e., skin irritation, acute toxicity and hemolysis activity) and solution properties of PDMS-g-CB (i.e., critical micelle concentration, CMC) were investigated. Due to the highly water-solubility of PDMS-g-CB, it's difficult to evaluate the antifouling properties of PDMS-g-CB directly, so they were blended with liquid silicones to give a PDMS-g-CB/PDMS blend film (b-PDMS) to examine the anti-fouling properties, in which PDMS-g-CB could be fixed on the surface of PDMS elastomer. Subsequently, the anti-fouling properties of PDMS-g-CB (resistance to protein adsorption and bacterial adhesion) were performed by b-PDMS indirectly.

2 EXPERIMENTAL

2.1 Materials

Octamethylcyclotetrasiloxane (D_4, > 99.5 %, Dow Corning, USA), 1, 3, 5, 7-tetramethylcyclo-tetrasiloxane (D^H_4, > 99 %, Hangzhou Silong Material Technology Co., Ltd, China) and hexamethyldisiloxane (MM, > 99 %, Dow Corning, USA) were dried before use. N, N-dimethylallylamino (DMAA, > 99 %, Haining City Huangshan Chemical Industry Co., Ltd, China) was purified by distillation before use. Platinum (0)-1, 3-divinyl-1, 1, 3, 3-tetramethyl-disiloxane complex solution (Karstedt's catalyst solution, Pt ~ 2 %, Aladdin Reagent Co. Ltd, China) was used as the catalyst of hydrosilylation. Purolite® CT175 (Purolite (China) Co. Ltd) is a clay containing sulphonic acid, it was used as received. Vinyl functionalized polysiloxanes (PMVS, Vi ~ 0.35 %, Dow Corning, USA) and sodium chloroacetate (SC, Aladdin Reagent Co., Ltd, China) were used as received. Other solvents, such as isopropanol, were used without any pretreatment. *Escherichia coli* (*E. coli*) was kindly supplied by the College of Natural Resources & Environment, South China Agricultural University.

2.2 Synthesis of PDMS-g-CB

In this paper, a series of carboxybetaine functionalized polysiloxanes (PDMS-g-CB) were synthesized via a three-step procedure (**Scheme 1**).

First of all, various hydrogen-containing polysiloxanes (PDMS-co-PHMS) with a relatively narrow molecular weight distribution were synthesized by the ring-opening polymerization of D_4 and D^H_4, and then N, N-dimethylallylamino (DMAA) was grafted to PDMS-co-PHMS via hydrosilylation reaction in the presence of Karstedt's catalyst to obtain PDMS-g-DMAA. Finally, carboxybetaine functionalized polysiloxanes (PDMS-g-CB) were prepared by subsequent quaternization reaction. (A detailed description can be found in the Supporting Information: Part **S1**)

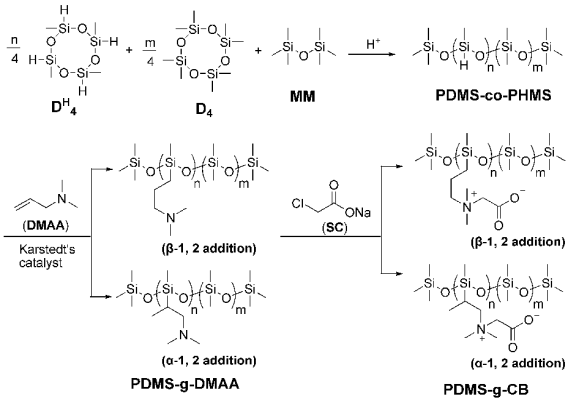

Scheme 1. The three-step synthesis routine of PDMS-g-CB.

2.3 Preparation of PDMS-g-CB blending PDMS film (b-PDMS)

To evaluate the hydrophilic properties and anti-fouling properties of PDMS-g-CB, a series of PDMS-g-CB were embedded into polydimethylsiloxanes elastomer (PDMS) by blending. Typically, vinyl functionalized polysiloxanes were mixed thoroughly with PDMS-g-CB / methanol solution (50 wt %), then hydrogen containing polysiloxanes (H wt % = 0.145 wt %, lab-made) and certain amount of Karstedt's catalyst were added. The homogeneous solutions were poured into a clean moulds coated with tetrafluoroethylene, then degassed under vacuum for 30 min. Films were cured at room temperature for 1 day. After curing, the b-PDMS films were peeled from the moulds carefully and cut into circular pieces (10 mm in diameter).

2.4 Structure characterization

Fourier transform infrared (FT-IR) spectra were recorded using a VERTEX-70 spectrometer (Brucker Instrument Corp., Germany) at resolution of 4 cm^{-1}, samples were coated on KBr plates and dried in the infrared lamp. The measurements were carried out over 400 - 4000 cm^{-1} range at room temperature. Attenuated total reflection fourier transform infrared (ATR-FTIR) spectra were measured on VERTEX-70 spectrometer equipped with a ATR accessory, 64 scans were collected for each sample.

^{1}H-NMR and ^{13}C-NMR spectra were collected with a Brucker Avance III-400 (400 MHz) fourier digital NMR spectrometer (Brucker Instrument Corp., Germany) at room temperature using $CDCl_3$ or D_2O as the solvent.

Gel permeation chromatography (GPC) was performed on an Elite EC2000 GPC apparatus (Dalian, China) equipped with a Shodex K-G guard column and a Shodex K-804L chromatographic column. Detection was achieved using a refractive index detector, and the samples were analyzed at 30 ºC

using $CHCl_3$ as the eluent at a flow rate of 1 mL / min. The instrument was calibrated using low polydisperse polystyrene standards.

The static water contact angles of PDMS-g-CB and b-PDMS surfaces were measured by a contact angle goniometer (JY-82, China) at room temperature. One drop of water (10 μL) was placed onto the surface with a proper pipette, and the water droplet was observed and recorded with an optical microscopy. More than three random positions were measured for each sample.

2.5 Determination of critical micelle concentration (CMC) of PDMS-g-CB

The CMC of PDMS-g-CB was determined by two commonly used methods, namely fluorescence probes and electrical conductivity methods. (A detailed description can be found in the Supporting Information: Part **S2**)

2.6 Antibacterial activity assessment

The antibacterial activities of PDMS-g-CB in different concentrations (15, 30 and 60 mg / mL) were evaluated by measuring the inhibition zones against *Escherichia coli* (*E. coli*), using the Agar well (Oxford cup) diffusion method. Briefly, 20 mL sterile nutrient agar was poured into sterile petri dishes with four sterile Oxford cups (inner diameter 6 mm), and 2 mL bacterial (*E. coli*) suspensions ($OD_{600} \approx 1.0$) were added into the dishes after the agar coagulated. Then PDMS-g-CB solutions with various concentrations, positive control (25 μg / mL of chloramphenicol) and negative control (sterile physiological saline) were added into each Oxford cup, respectively. All the dishes were incubated at 37 ºC for 24 h, and the inhibition zones were measured and recorded.

2.7 Skin irritation testing

Evaluation of the potential for PDMS-g-CB to cause skin irritation was conducted in rabbits *in vivo* according to ISO 10993-10: 2002. (A detailed description can be found in the Supporting Information: Part **S3**)

2.8 Acute oral toxicity testing

In order to assess the toxicity of PDMS-g-CB, the acute oral toxicity (LD_{50} as the index) was determined using NIH mice (22 ~ 25g), according to the OECD Acute Oral Toxicity Test Guideline 425 procedure (OECD TG 425). (A detailed description can be found in the Supporting Information: Part **S4**)

2.9 Hemolysis assay

Hemolysis assay was performed with fresh rabbit blood obtained from a New Zealand white rabbit, according to ISO 10993-4: 2002. (A detailed description can be found in the Supporting Information: Part **S5**)

2.10 Protein adsorption

Bovine serum albumin (BSA) was used as the model protein for evaluation of protein adsorption. To measure the amounts of protein adsorbed onto PDMS and b-PDMS surfaces, the films were immersed in 10 mL protein solutions (BSA, 4 mg / mL) and incubated at 37 ºC for 60 min, then the films were removed from the BSA solution and rinsed with PBS for three times. Subsequently, the films were sonicated for 120 min in PBS to detached the protein adsorbed onto native PDMS and b-PDMS surfaces, then the solution was collected and the amount of protein was determined by the Micro BCA (bicinchoninic acid) Protocol (Micro BCA Protein Assay Kit, Sangon Biotech Co., Ltd., Shanghai, China) [26, 27]. Afterwards, the amount of adsorbed protein was calculated according to the standard protein curve, which was measured with different concentration of protein standard.

2.11 Bacterial adhesion

Escherichia coli (*E. coli*) was used to investigate the bacterial adhesion behaviours on the surface of native PDMS and b-PDMS films. *E. coli* was incubated in a broth medium (containing 3.0 mg / mL beef extract, 10.0 mg/mL peptone and 5.0 mg / mL sodium chloride) at 37 ºC for 24 h. The bacterial concentration was measured by spectrophotometer at 540 nm (OD_{540}) with the assumption that the $OD_{540} = 1.0$ is corresponding with a bacterial concentration of approximately 10^9 colony-forming units (CFU) per millilitre [28]. For the antibacterial assay, the *E. coli* containing broth was washed and re-suspended in PBS to obtain a bacterial suspension, which has a concentration of 10^8 CFU / mL. The native PDMS and modified PDMS (b-PDMS) were sterilized with ultraviolet rays (each side for 30 min) and then immersed in the bacterial suspension in a sterile flask, which was cultured at 37 ºC for 20 h. Afterwards, the films were removed and rinsed three times for 10 min in sterile PBS, and bacteria adhered onto the surface was immobilized with 2.5 % glutaraldehyde solution for 6 h at 4 ºC. Then the films were washed with sterile PBS for three times, and dehydrated step by step in a series of ethanol/water mixtures (30 %, 50 %, 70 %, 80 %, 95 % and 100 % by volume, 20 min for each). Finally, the dried films was coated with gold and observed with a scanning electron microscopy (Zeiss EVO 18, Germany).

3 RESULTS AND DISCUSSION

3.1 Synthesis and characterization PDMS-g-CB

A series of PDMS-g-CB with different carboxybetaine grafting ratio were prepared via a three-step process (ring-opening polymerization, hydrosilylation reaction and quaternization reaction) as described in **Scheme 1**. The chemical structures of stage products were confirmed by FT-IR and ^{1}H-NMR spectroscopy.

It is well known that hydrogen-containing polysiloxanes can be prepared by the ring-opening polymerization (ROP) of cyclosiloxanes or condensation of linear siloxanes, [29, 30] and researchers found that the hydrogen content and molecular weight of resulting polymer is more controllable via ROP of cyclosiloxanes. As reported previous, [25] PDMS-co-PHMS was synthesized by the cationic ring-opening polymerization of D_4, D^H_4 and MM using strong acid ion exchange resin (Purolite ® CT175) as the catalyst, the hydrogen content and molecular weights of PDMS-co-PHMS were controlled by adjusting the mole ratio of D_4, D^H_4 and end-agent (MM). The structures of PDMS-co-PHMS were characterized by FT-IR and ^{1}H-NMR. Representative FT-IR spectra of PDMS-co-PHMS are shown in **Figure 1**, the absorption peaks at 2962, 2158, 1261, 1093, 1010 and 802 cm^{-1} are corresponding to the stretching vibration of C-

H, Si-H, Si-CH_3 and Si-O-Si, respectively. And the intensity of Si-H absorption peak increase with the increment of D^H units. **Figure 2** shows the classic ^{1}H-NMR spectra of PDMS-co-PHMS, the characteristic signal of Si-H protons appeared at δ = 4.7 ppm, and the signal at δ = 0 ~ 0.2 ppm attributed to the protons in Si-CH_3. The molecular weight and hydrogen content of various PDMS-co-PHMS were measured with GPC and ^{1}H-NMR (as shown in **Table S1**), which indicated that the molecular weight of PDMS-co-PHMS is close to the theoretical value calculated from the designed molecular formula.

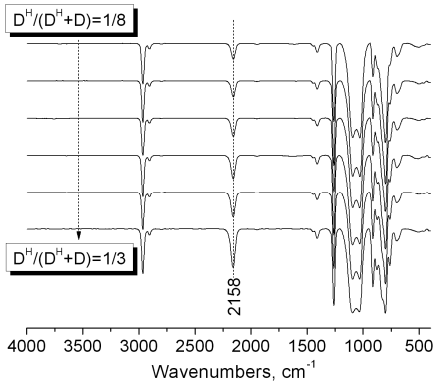

Figure 1. The FT-IR spectra of PDMS-co-PHMS of various compositions.

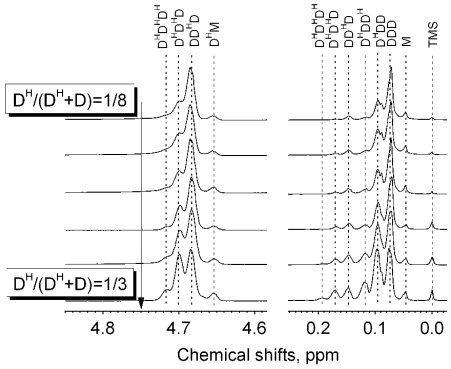

Figure 2. The ^{1}H-NMR spectra of PDMS-co-PHMS of various compositions.

In the second step of PDMS-g-CB synthesis, tertiary amino functionalized group were introduced into the siloxanes backbone via the hydrosilylation reaction, which is the most important methodology for the synthesis of organo-functionalized siloxanes in silicone chemistry. Hydrosilylation reaction refers to an addition reaction of Si-H bonds to unsaturated bonds such as C=C, the addition process in principle could occur in two directions to give α-1, 2 and β-1, 2 addition products, as shown in **Scheme 2**. The course of addition has been proven to depend on the structure of unsaturated monomer, the temperature and the catalyst. [31]

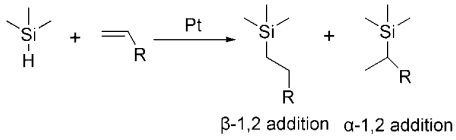

Scheme 2. Two possible hydrosilylation patterns of Si-H containing siloxanes.

Herein, PDMS-g-DMAA was synthesized by the hydrosilylation reaction of PDMS-co-PHMS with DMAA in the presence of Karstedt's catalyst. The progress of hydrosilylation reactions were traced by the variation of characteristic Si-H absorption at 2158 cm^{-1} by FT-IR. **Figure 3** represents the FT-IR spectra of PDMS-co-PHMS and PDMS-g-DMAA, the Si-H absorption band at 2158 cm^{-1} and 912 cm^{-1} disappeared completely demonstrating the effectiveness of hydrosilylation reaction, and the absorption bands observed at 2816 cm^{-1} and 2764 cm^{-1} are due to the introduction of -$N(CH_3)_2$ groups. The completion of hydrosilylation reaction was confirmed by ^{1}H-NMR spectra (**Figure 4**), which presented the disappearance of Si-H group (characteristic signal at δ = 4.7 ppm) and appearance of a series of C-H protons. Besides, the ^{1}H-NMR spectrum of PDMS-g-DMAA indicated that both α-1, 2 addition products and β-1, 2 addition products were obtained in the hydrosilylation of PDMS-co-PHMS and DMAA, because the characteristic signal of methyl protons which are connected to -CCH_2-$N(CH_3)_2$ can be observed at about 1.0 ppm (α-1, 2 addition pattern). The two addition patterns of hydrosilylation reaction could also be conformed by the ^{13}C-NMR spectrum (**Figure 5**). The proportion of α-1, 2 addition products and β-1, 2 addition products calculated from the ^{1}H-NMR spectrum was about 25% and 75%, respectively.

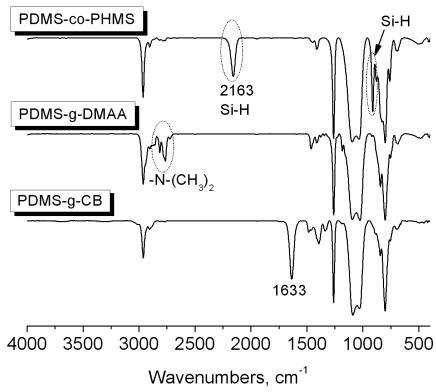

Figure 3. The FT-IR spectra of PDMS-co-PHMS, PDMS-g-DMAA and PDMS-g-CB.

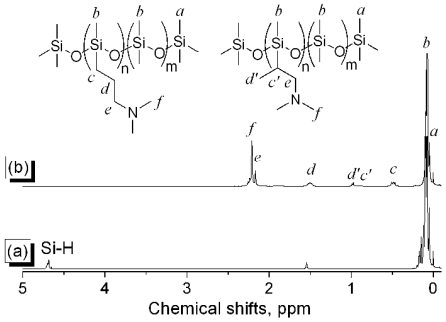

Figure 4. The ^{1}H-NMR spectra of (a) PDMS-co-PHMS and (b) PDMS-g-DMAA (in $CDCl_3$).

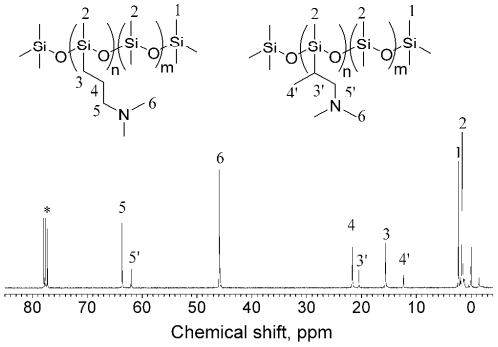

Figure 5. The ^{13}C-NMR spectrum of PDMS-g-DMAA (in $CDCl_3$).

The tertiary amino functionalized polysiloxanes were then allowed to react with sodium chloroacetate (SC) to give generation of carboxybetaine functionalized polysiloxanes. The substances (PDMS-g-CB) were isolated as faint yellow solids, which are fairly hygroscopic and soluble in polar solvents such methanol, ethanol, isopropanol and water. **Figure 3** shows the FT-IR spectrum of PDMS-g-CB, there is a new absorption band at 1633 cm^{-1} compared with the spectrum of PDMS-g-DMAA, which is attributed to the C=O stretching vibration of a carboxylate group. Another change in the FT-IR spectra is the disappearance of -$N(CH_3)_2$ absorption bands at about 2800 cm^{-1}, it revealed that the tertiary amino groups have been converted into quaternary ammonium groups completely. **Figure 6** shows the ^{1}H-NMR spectrum of PDMS-g-CB, which indicated that the structure of resulting compound agree well with expectation. After the quaternization reaction, the characteristic protons signals of -$N(CH_3)_2$ group at about 2.2 ppm shift to 3.2 ppm completely, it also demonstrated that the tertiary amino groups have been converted to quaternary ammonium groups.

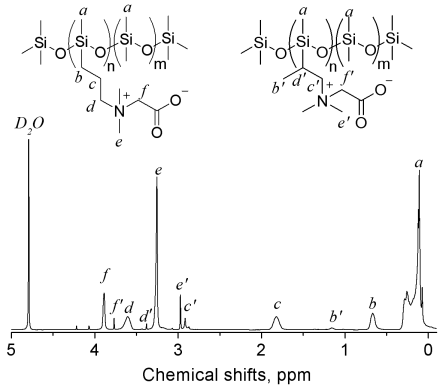

Figure 6. ^{1}H-NMR spectrum of PDMS-g-CB (in D_2O).

3.2 Surface characterization of b-PDMS films

b-PMDS films were prepared by blending PDMS-g-CB with liquid silicones which would be cross-linked in the presence of Pt catalyst. Surface structure analysis of b-PDMS films was performed with ATR-FTIR. **Figure 7** shows the typical ATR-FTIR spectra of native PDMS and b-PDMS (0.5 wt%, 1 wt% and 2 wt% PDMS-g-$CB_{1/3}$, respectively), in which the characteristic signal of the carboxylate group at about 1633 cm^{-1} can't be observed in the native PDMS spectrum but appears in all spectra of b-PDMS, it indicated that PDMS-g-CB had been blended into polydimethylsiloxanes elastomer successfully. Besides, with the increase of the content of PDMS-g-$CB_{1/3}$, the peak intensity of C=O bonds also increase, which revealed that the amount of PDMS-g-CB on the surface of PDMS is depend on the concentration of blending PDMS-g-CB.

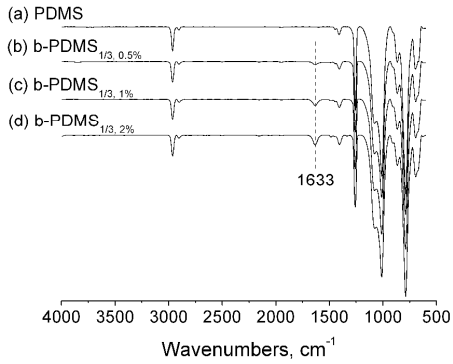

Figure 7. ATR-FTIR spectra of PDMS-g-$CB_{1/3}$ blending PDMS: (a) 0%, (b) 0.5%, (c) 1%, (d) 2%.

The water contact angles on the surfaces of native PDMS and b-PDMS were measured to characterize the hydrophilic properties of b-PDMS. The detailed contact angles measurement results are shown in **Figure 8**. After blending PDMS with PDMS-g-CB, the contact angles of these modified surfaces were decreased significantly, and the contact angle decrease slightly while the content of PDMS-g-CB increase. The decrease of water contact angles are attributed to the introducing of hydrophilic carboxybetaine groups on the surfaces of PDMS.

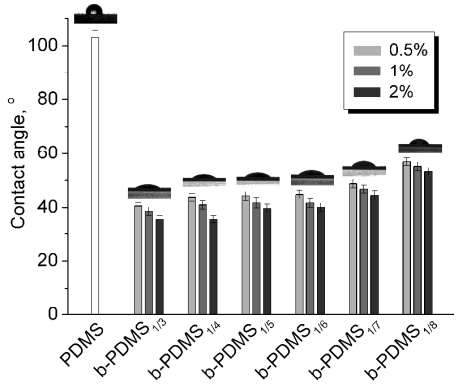

Figure 8. Static water contact angle of PDMS-g-CB blending PDMS. (The images inserted on the bars are the water contact angle photos for PDMS and b-$PDMS_{1\%}$, respectively.)

3.3 Determination of CMC

As a kind of zwitterionic polymer, PDMS-g-CB contains a hydrophobic backbone and several zwitterionic short side chain, thus it could be considered as zwitterionic surfactant, and its critical micelle concentration (CMC) was concerned. Here, the CMC values of various grafting ratio were investigated by fluorescence probes and electrical conductivity methods, respectively.

Fluorescence probe technique has been used in the study of surfactant micelles for many years, the so-called pyrene 1 : 3 ratio method are useful for determination of CMC values and aggregation number of micelles. [32, 33] The typical excitation spectra of PDMS-g-CB solutions at different concentrations are

presented in **Figure 9**. It is noticed that the intensity increasing with the concentration of PDMS-g-CB, and the intensity ratio (I_1 / I_3) of first (λ = 373 nm) and third vibrational bands (λ = 384 nm) also changes with the polymer concentration. Those changes were attributed to the environment change of pyrene molecules, they transfer from water environment to the hydrophobic micelle while the micelles were formed. Thus we could determinate the CMC values from the relationship between I_1 / I_3 and polymer concentration. **Figure S1** shows the pyrene fluorescent intensity ratio (I_1/I_3) as a function of various concentrations of PDMS-g-CB with different carboxybetaine grafting ratio (1/3 ~ 1/8). The CMC values of PDMS-g-CB were estimated by the intersection of the two tangent of I_1 / I_3 ratio ~ log C curve as shown in **Figure S1** and the results were presented in **Figure 10**.

We also measured the CMC values of PDMS-g-CB by the common conductance method. [34] **Figure S2** show the conductivity plots for PDMS-g-CB with different carboxybetaine grafting ratio, and **Figure 10** summarizes the results of CMC values calculated from the curves in **Figure S2**.

As can be seen from **Figure 10**, The CMC values of PDMS-g-CB vary from 30 mg / L to 80 mg / L, which are even lower than the commonly used sodium dodecyl sulfate surfactant (SDS, CMC ~ 80 mg / L at 25 ºC). [35] The low CMC of PDMS-g-CB was attributed to the high hydrophobicity of siloxane backbone. Besides, the CMC values increased with the grafting ratio of carboxybetaine groups, the change may be affected by the hydrophilicity of the grafting zwitterionic carboxybetaine.

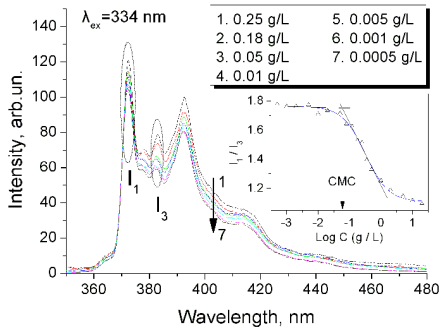

Figure 9. Fluorescence spectra of pyrene (6×10^{-7} M) in aqueous solutions of PDMS-g-$CB_{1/7}$ at different concentrations.

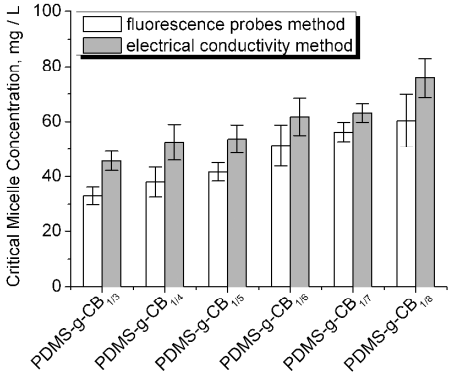

Figure 10. The CMC values of various proportions of PDMS-g-CB.

3.4 Hemolytic properties of PDMS-g-CB blending PDMS

When biomaterials were exposed to blood, coagulation may be caused by the detrimental interaction between the surfaces of materials and blood constituents. To evaluate the hemolytic properties of b-PDMS and PDMS-g-CB, a hemolysis test was carried out in vitro using fresh rabbit blood under static conditions. And the hemolysis of red blood cells (RBC) suspension in distilled water and physiological saline was used as positive control and negative control, respectively. **Figure 11** shows the hemolytic activities of b-PDMS with different content of PDMS-g-$CB_{1/3}$, where the hemolysis ratio of PDMS and b-PDMS were much lower than 5%, which indicated that the blending additive (PDMS-g-CB) also had no hemolytic effect on the RBC suspension.

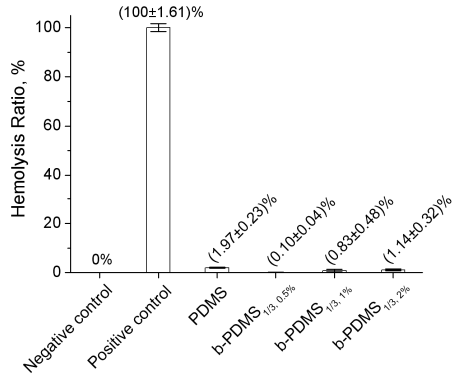

Figure 11. The results of hemolysis test for native PDMS and b-$PDMS_{1/3}$ film.

3.5 Antibacterial properties of PDMS-g-CB

To evaluate the antibacterial properties of PDMS-g-CB, different concentrations of PDMS-g-CB solutions were added to the *E.coli* cultures using the Agar well (Oxford cup) diffusion method, and the antibacterial properties were assessed by measuring inhibition zones. The diameter of inhibition zones of PDMS-g-CB with different concentrations were recorded in **Figure 12** and **Figure S6**. Results show that the inhibition zones of PDMS-g-CB were about 7 mm and almost the same with negative control. It indicated that PDMS-g-CB have no antibacterial activity towards *E. coli*, which conforms to the result of Jiang and co-workers. [36]

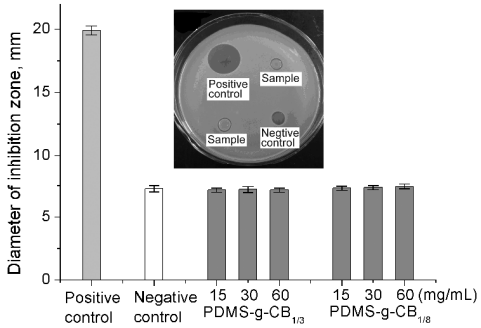

Figure 12. Antibacterial activity of different concentrations of PDMS-g-CB against *E. coli*. (The insert image is the antibacterial results for PDMS-g-$CB_{1/3}$, at 30 mg / mL)

3.6 Evaluation of skin irritation of PDMS-g-CB

As PDMS-g-CB may contact with the skin of human or animals in application, we evaluated the skin irritant and sensitization reactions of PDMS-g-CB. Testing for skin irritation of PDMS-g-

CB has been performed on rabbits, and the results are shown in **Table 1** and **Figure S4**. The results suggested that no skin irritation was caused by PDMS-g-CB. In addition, no significant change was observed in the body weight of test rabbits, and no signs of intoxication were found. As a result, PDMS-g-CB is a kind of novel material with no skin irritation.

Table 1. The evaluation of skin irritation of PDMS-g-CB

Samples	Mean irritation score				Irritation Index [a]	Intensity
	1 h	24h	48h	72h		
PDMS-g-$CB_{1/3}$	0	0	0	0	0	no irritation
PDMS-g-$CB_{1/8}$	0	0	0	0	0	no irritation
Gauze	0	0	0	0	0	no irritation
Physiological Saline	0	0	0	0	0	no irritation

a. Irritation Index = (Σ erythema grades of 24/48/72 h + Σ oedema grades of 24/48/72 h) / (3×number of rabbits).

3.7 Acute oral toxicity study

The toxicities of PDMS-g-CB were investigated by acute oral toxicity test at a dose of 5000 mg/kg according to OECD guidelines 425 (OECD TG 425). After feeding for 7 days and 14 days, no abnormal behaviours and adverse reaction were observed in the experimental group mice compared with the control group, and the weight of the experimental group mice and control group mice had no significant difference. During the observation period, no death was noted both in control and experimental groups (**Table 2**). In addition, the histopathological effect of PDMS-g-CB on organs (heart, liver, spleen, lung and kidney) was observed by light microscopy (**Figure S5**), it's noticed that no histopathological changes were observed both in the experimental groups and control group, so PDMS-g-CB has no significant toxicity on the organs (good histocompatibility). Therefore, the oral LD_{50} of PDMS-g-CB was determined to be greater than 5000 mg/kg, the result revealed that PDMS-g-CB could be consider as practically non-toxic classification.

Table 2. The survival state of mice after acute toxicity test of PDMS-g-$CB_{1/3}$

	Dosage (mg/kg)	Number of death (n = 8)						Percentage survival (%)
		12 h	1 d	2 d	3 d	7 d	14 d	
Control Group	0	0	0	0	0	0	0	100
Experimental Group	5000	0	0	0	0	0	0	100

3.8 Protein adsorption of b-PDMS films

It is believed that most undesired bio-adsorption and bio-fouling on the surfaces of materials are promoted by protein adsorption. Therefore, protein resistance is the primary target for construction of low-fouling or non-fouling surface. Herein, we chose BSA, extensively existing in blood and plasma, as the model protein for protein adsorption testing. **Figure 13** shows the amount of BSA adsorbed onto the surfaces of native PDMS and PDMS-g-CB blending PDMS (b-PDMS), which were calculated according to the micro-BCA method. It was noticed that the amount of adsorbed BSA decreased drastically after modification with PDMS-g-CB, and the amount of adsorbed BSA on b-PDMS surfaces decreased slightly while the carboxybetaine grafting ratio of PDMS-g-CB increased. The results agree well with the water contact angle data as shown in **Figure 8**. When PDMS was modified with zwitterionic polymer, the zwitterionic polymer could form a hydration layer on the surface, [23] which would prevent the adsorption of protein. Therefore, the more carboxybetaine groups on the modified PDMS surface, the more efficient for resistance of protein adsorption. And it explained that why less BSA adsorbed on the b-$PDMS_{1/3}$ surface compared with b-$PDMS_{1/8}$ surface.

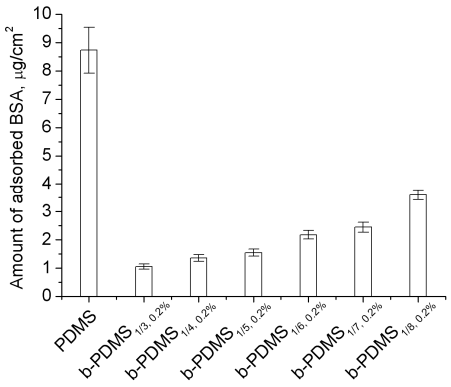

Figure 13. Amount of protein adsorbed onto the surface of PDMS-g-CB blending PDMS.

3.9 Bacterial adhesion of b-PDMS films

The adhesion of bacteria onto materials is an essential factor leading to biofilm formation and infection. To construct a low-fouling surface, it's necessary to reduce or inhibit the adhesion of bacteria. In our work, short-term (24 h) adhesion of *E. coli* onto b-PDMS surfaces with various content of zwitterionic polymers were investigated, using native PDMS as a control. The adhering bacteria on the materials surfaces were visualized by SEM, **Figure 14** shows the representative image of native PDMS and b-PDMS after bacterial adhesion. In **Figure 14**-A1 and A2, numerous bacteria can be observed on the surface of native PDMS (untreated PDMS). The number of bacteria on the b-PDMS surface (**Figure 14**-B-G) were significantly less than the native PDMS surface. After counting the exactly number of 10 pieces SEM images for each sample, the average number of adsorbed bacterial was shown in **Figure 15**. It could be found that the higher content of PDMS-g-CB is, the less adhering bacteria there are; besides, the number of adhering bacteria decreased slightly when the carboxybetaine grafting ratio of PDMS-g-CB increased. It was noticed that the number of adhering bacteria has close relationship with the hydrophilicity of surface, the more hydrophilic the surface is, the less bacteria adhere onto it, which was consistent with what Jansen [37] and Kodjikian had reported [38]. The results of bacterial adhesion test reveal that PDMS-g-CB modified surfaces could resist the adhesion of *E. coli* effectively, which is highly desired for the construction of anti-fouling surfaces.

Cite this: DOI:

www.rsc.org/advances

Full Paper

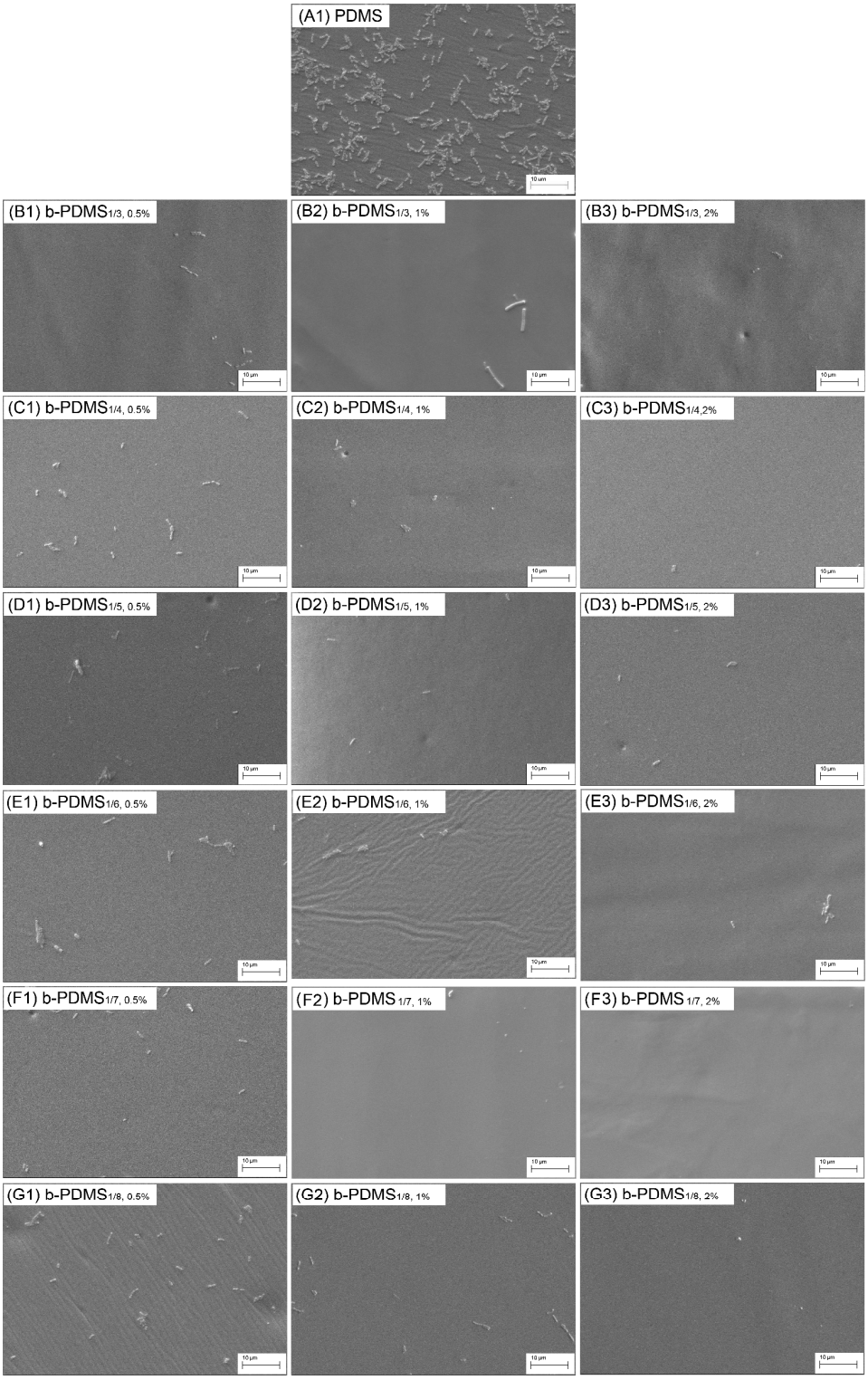

Figure 14. SEM images of the surfaces of native PDMS and b-PDMS with different content of PDMS-g-CB after the short-term bacterial (*E. coli*) adhesion.

Cite this: DOI:

www.rsc.org/advances

Full Paper

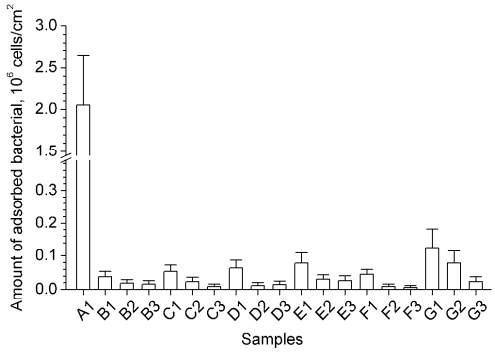

Figure 15. The average bacterial adsorption on the sample surface calculated from the SEM images. (Samples A1 to G3 has the same meaning with the captions listed in Figure 14)

4. CONCLUSION

In this study, a series of novel carboxybetaine functionalized polysiloxanes (PDMS-g-CB), composed of a siloxane backbone hydrophobic portion and a carboxybetaine hydrophilic portion, were synthesized and characterized. PDMS-g-CB exhibited a low CMC, water-soluble, no antibacterial activity, no skin irritation, non-toxic and good biocompatibility. And PDMS-g-CB modified PDMS films (b-PDMS) show highly resistance to protein adsorption and bacterial adhesion, regardless of the grafting ratio of carboxybetaine groups in PDMS-g-CB. Therefore, PDMS-g-CB is an environmentally friendly material with excellent anti-fouling properties.

ACKNOWLEDGMENTS

The authors acknowledge financial support from the National Natural Science Foundation of China (grants 31201552 and 51003032) and the Specialized Research Fund for the Doctoral Program of Higher Education (grant 20124404120025).

Notes and references

[a] *Department of Polymer Material Science and Engineering, College of Material Science and Engineering, South China University of Technology, 381 Wushan Rd., Guangzhou 510641, Guangdong, China Fax/Tel: 011-86-20-87112466; E-mail: aqzhang@scut.edu.cn*

[b] *Department of Pharmaceutical Engineering, College of Natural Resource and Environment, South China Agriculture University, 483 Wushan Rd., Guangzhou 510642, Guangdong, China. E-mail: linyaling@scau.edu.cn*

† Electronic Supplementary Information (ESI) available: [Synthesis detail of PDMS-g-CB, determination of CMC, skin irritation, acute oral toxicity testing, hemolysis assay and antibacterial activities of PDMS-g-CB.]. See DOI:

1 M. E. Gray. *J Agr Food Chem*, 2010, **59**, 5852.
2 M. Perugini, M. Cavaliere, A. Giammarino, P. Mazzone, V. Olivieri and M. Amorena. *Chemosphere*, 2004, **57**, 391.
3 P. Christou, T. Capell, A. Kohli, J.A. Gatehouse and A.M. Gatehouse. *Trends Plant Sci*, 2006, **11**, 302.
4 O. Lopez, J. G. Fernandez-Bolanos, M. V. Gil. *Green Chem*, 2005, **7**, 431.
5 D. R. Walters. *Eur J Plant Pathol*. 2006, **114**, 255.
6 F. Jin, B. Z. Ji, S. W. Liu, L. Tian, J. Gao. *Acta Entom. Sin.*, **2009**, 52, 1008.
7 H. G. Silverman, F. F. Roberto. *Mar Biotechnol*, 2007, **9**, 661.
8 M. F. A. Goosen, S. S. Sablani, H. Ai-Hinai, S. Ai-Obeidani, R. Al-Belushi, D. Jackson. *Sep Sci Technol*, 2005, **39**, 2261.
9 P. Kingshott, H. Thissen, H. J. Griesser. *Biomaterials*, 2002, **23**, 2043.
10 P. Harder, M. Grunze, R. Dahint, G. M. Whitesides, P. E. Laibinis. *J Phys Chem B*, 1998, **102**, 426.
11 B. Thierry, L. Zimmer, S. McNiven, K. Finnie, C. Barbe, H. J. Griesser. *Langmuir*, 2008, **24**, 8143.
12 P. Gong, D. W. Grainger. *Methods Mol Biol*, 2007, **381**, 59.
13 L. Li, S. Chen, J. Zheng, B. D. Ratner, S. Jiang. *J Phys Chem B*, 2005, **109**, 2934.
14 J. Zheng, L. Li, H. K. Tsao, Y. J. Sheng, S. Chen, S. Jiang. *Biophys J*, 2005, **89**, 158.
15 D. A. Herold, K. Keil, D. E. Bruns. *Biochem pharm*, 1989, **38**, 73.
16 E. Ostuni, R. G. Chapman, R. E. Holmlin, S. Takayama, G. M. Whitesides. *Langmuir*, 2001, **17**, 5605.
17 Z. Cao, S. Jiang. *Adv Mater*, 2010, **22**, 920.
18 J. Ladd, Z. Zhang, S. Chen, J. C. Hower, S. Jiang. *Biomacromolecules*, 2008, **9**, 1357.
19 R. E. Holmlin, X. Chen, R. G. Chapman, S. Takayama, G. M. Whitesides. *Langmuir*, 2001, **17**, 2841.
20 G. Cheng, G. Li, H. Xue, S. Chen, J. D. Bryers, S. Jiang. *Biomaterials*, 2009, **30**, 5234.
21 L. R. Carr, H. Xue, S. Jiang. *Biomaterials*, 2011, **32**, 961.
22 W. Yang, H. Xue, L. R. Carr, J. Wang, S. Jiang. *Biosens Bioelectron*, 2011, **26**, 2454.
23 S. Chen, L. Li, C. Zhao, J. Zheng. *Polymer*, 2010, **51**, 5283.
24 Y. He, J. Hower, S. Chen, M. T. Bernards, Y. Chang, S. Jiang. *Langmuir*, 2008, **24**, 10358.
25 L. Cheng, Q. Liu, L. Yang, Y. Lin, A. Zhang. *Polym Mat Sci Engi*, 2014, **30**, 25. (In Chinese)
26 K. Ishihara, A. Fujiike, Y. Iwasaki, K. Kurita, N. Nakabayashi. *J Polym Sci Part A Polym Chem*, 1996, **34**, 199.
27 S. Fujishita, C. Inaba, S. Tada, H. Kitano, M. Gemmei-Ide, Y. Saruwatari. *Biol Pharm Bull*, 2008, **31**, 2309.
28 A. H. Hogt, J. Dankert, J. Feijen. *J Biomed Mater Res*, 1986, 20, 533.
29 A. Saxena, M. Markanday, A. Sarkar, V. K. Yadav, A. S. Brar. *Macromolecules*, 2011, **44**, 6480.
30 X. Hao, J. L. Jeffery, J. S. Wilkie, G. F. Meijs, A. B. Clayton, J. D. Watling, A. Ho, V. Fernandez, C. Acosta, H. Yamamoto, M. G. M. Aly, J. M. Parel, T. C. Hughes. *Biomaterials*, 2010, **31**, 8153.
31 E. Lukevics, L. E. Demicheva, N. P. Yerchak, Y. Popelis. *Russ Chem Bull*, 1993, **42**, 1709.
32 J. Aguiar, P. Carpena, J. A. Molina-Bolívar, R. C. Carnero. *J Colloid Interf Sci*, 2003, **258**, 116.
33 I. Astafieva, X. Zhong, A. Eisenberg. *Macromolecules*, 1993, **26**, 7339.
34 A. Dominguez, A. Fernandez, N. Gonzalez, E. Iglesias, L. Montenegro. *J Chem Edu*, 1997, **74**, 1227.
35 A. Shiloach, D. Blankschtein. *Langmuir*, 1998, **14**, 7166.
36 Z. Zhang, G. Cheng, L. R. Carr, H. Vaisocherova, S. Chen, S. Jiang. *Biomaterials*, 2008, **29**, 4719.
37 B. Jansen, G. Peters. *J Hosp Infect*. 1991, **19**, 83.
38 L. Kodjikian, C. Burillon, C. Roques, G. Pellon, J. Freney, F. N. R. Renaud. *Invest Ophth Vis Sci*, 2003, **44**, 4388.